

Bursts in average lifetime of transients for chaotic logistic map with a hole

Paar, Vladimir; Pavin, Nenad

Source / Izvornik: **Physical Review E, 1997, 55, 4112 - 4115**

Journal article, Published version

Rad u časopisu, Objavljena verzija rada (izdavačev PDF)

<https://doi.org/10.1103/PhysRevE.55.4112>

Permanent link / Trajna poveznica: <https://urn.nsk.hr/urn:nbn:hr:217:033675>

Rights / Prava: [In copyright](#) / [Zaštićeno autorskim pravom.](#)

Download date / Datum preuzimanja: **2024-04-19**



Repository / Repozitorij:

[Repository of the Faculty of Science - University of Zagreb](#)



Bursts in average lifetime of transients for chaotic logistic map with a hole

V. Paar and N. Pavin

Department of Physics, Faculty of Science, University of Zagreb, Zagreb, Croatia

(Received 30 October 1996)

Chaotic transients are studied for a logistic map at $r=4$, with an inserted narrow hole. We find that average lifetime τ of chaotic transients that are dependent on the hole position roughly follows the Frobenius-Perron semicircle pattern in most of the unit interval, but at the positions that correspond to the low period $(1,2,3, \dots)$, unstable periodic orbits of the logistic map at $r=4$ there are bursts of τ . An asymptotic relation between the Frobenius-Perron and Kantz-Grassberger average lifetimes, at these positions, is obtained and explained in terms of missing preimages determined from a transient time map. The addition of noise leads to the destruction of bursts of average lifetime. [S1063-651X(97)11204-1]

PACS number(s): 05.45.+b

A transiently chaotic trajectory looks chaotic up to a certain time and then switches into a nonchaotic behavior that governs the rest of the trajectory [1]. Transient chaos plays an important role in nonlinear systems. It was first observed in the Lorenz model [2–4] and subsequently found in different kinds of nonlinear systems, for example, in low-dimensional maps [5–10], nonlinear oscillators [11], coupled map lattices [12,13], etc. Of particular importance was the discovery that chaotic transients appear in dynamical systems passing through crises [14] and characterizations of natural measure on repellers [15–20].

In one-dimensional maps, transient chaos occurs if a unit interval I is mapped under the dynamics $f(x)$ not only onto itself but also partially outside itself [1]. It is irrelevant how the map looks for x values outside I , because there is no feedback from these regions. A typical example of such a map is the famous logistic map $x_{n+1}=f(x_n)$, where $f(x)=rx(1-x)$ [19–23] in the case where control parameter r is larger than 4. In that case almost all orbits escape from the unit interval I through the gap at the vertex of parabola and the invariant set is a repelling Cantor set in I [1,8].

The logistic map at $r=4$ maps the unit interval I onto itself [21,22].

In this paper we investigate the map producing chaotic transients defined on the unit interval I by

$$f(x) = \begin{cases} 4x \times (1-x), & x \notin I^{(0)} \\ \infty, & x \in I^{(0)}, \end{cases} \quad (1)$$

where $I^{(0)}$ is a narrow interval $(\xi - (d/2), \xi + (d/2))$ within I . This map coincides with the logistic map at $r=4$ except for a narrow hole in the interval $I^{(0)}$ of width d at position $x=\xi$ (Fig. 1).

In the unit interval I , the logistic map at $r=4$ is chaotic, but with many embedded unstable periodic orbits: one period-1 orbit, one period-2 orbit, two period-3 orbits, three period-4 orbits, six period-5 orbits, etc. [20].

In an analogy to the case of the logistic map at $r>4$ [20], the interval $I^{(0)}$ represents a loss region through which the orbit initially in the unit interval I can leak out. The orbits for the map (1) in the unit interval I are similar to those of the

logistic map at $r=4$, until they fall in the loss region. In the first iteration, the interval $I^{(0)}$ around ξ escapes; in the second iteration, its preimages escape; and so on. Finally, the invariant set in I is a chaotic repeller.

A basic difference of the map (1) with respect to the previously studied single-humped one-dimensional maps [1,8] should be noted: in the latter case the number of successive preimages of the interval corresponding to $f(x)>1$ increases as 2^n , while for the map (1) some subsets of preimages of the interval $I^{(0)}$ are missing, depending on position of the hole.

An important question concerning the chaotic map (1) is the following: what is the average lifetime τ of chaotic transients for a set of a large number of initial positions x_0 , uniformly distributed in the unit interval I ?

Employing first the Frobenius-Perron equation, we have [19]

$$\left[1 - \int_{\xi-d/2}^{\xi+d/2} \frac{1}{\pi \sqrt{x(1-x)}} dx \right]^\tau = \frac{1}{e}. \quad (2)$$

From this expression we calculate dependence of the average lifetimes τ , which are shown in Fig. 2, on the hole position ξ for a fixed width $d=0.01$ (dashed line). In accordance with

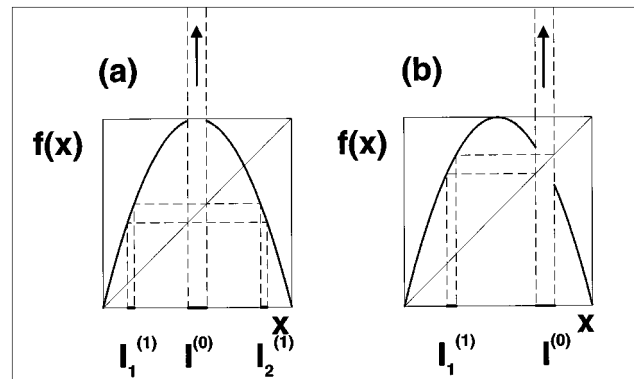


FIG. 1. Logistic map at $r=4$ with an additional hole of width d at the position ξ on the unit interval [Eq. (1)]. As an illustration, the hole position is (a) $\xi=0.5$, (b) $\xi=0.75$, and the hole width is $d=0.1$. Only the first order preimages are shown. Observe that the preimage $I_2^{(1)}$ is missing for $\xi=0.75$.

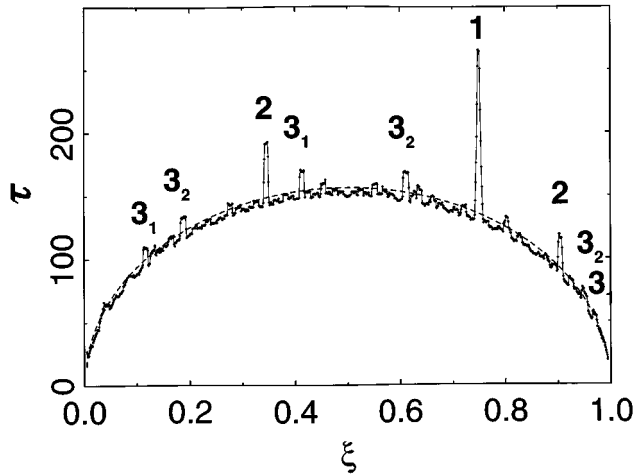


FIG. 2. Average lifetime τ of chaotic transients associated with map (1) depending on the hole position ξ (solid circles). The width of the hole d is kept fixed at $d=0.01$. In each case the average lifetime is obtained from exponential decay of trajectories, starting from the set of 10^6 initial positions uniformly distributed over the unit interval. One unit of average lifetime corresponds to one iteration step. Classification number k , corresponding to the period of the corresponding unstable periodic orbits for the logistic map at $r=4$, is assigned to pronounced peaks (see the text). Dashed and solid lines correspond to Frobenius-Perron and Kantz-Grassberger equations, respectively (see the text).

its stochastic character, the Frobenius-Perron equation gives a smooth semicirclelike pattern.

On the other hand, we directly calculate the average lifetime for each of the hole positions $\xi=0.5d, 0.6d, 0.7d, \dots, 1-0.5d$ along the unit interval, where the intervals of the neighboring holes overlap. In each case, the average lifetime τ was determined from an exponential decay of the number of survivors [1]. The calculated average lifetimes are shown in Fig. 2 (solid circles connected by a solid line). In a sizeable fraction of the unit interval, the gross behavior of the calculated average lifetime is well approximated by the Frobenius-Perron equation, but at some positions there appear narrow bursts of average lifetime, sizeably exceeding the Frobenius-Perron prediction (2). The largest peak $\tau_1=1.95\tau_{FP}$ [τ_{FP} denotes solutions of Eq. (2)] is obtained for the hole position $\xi=0.75$, which corresponds to the position of the period-1 unstable orbit of the logistic map at $r=4$. This peak is associated with the classification number $k=1$. The second pronounced group of two peaks is obtained at the hole positions $\xi=(5-\sqrt{5})/8=0.345$ and $\xi=(5+\sqrt{5})/8=0.904$, which correspond to the positions of the period-2 orbit of the logistic map at $r=4$. The corresponding average lifetimes are $\tau_2=1.29\tau_{FP}$ and $\tau_2=1.26\tau_{FP}$, respectively. These two peaks are associated with the classification number $k=2$. The third group of six peaks, associated with the classification number $k=3$, corresponds to the holes at 0.117, 0.413, 0.970, 0.188, 0.611, and 0.950. In these cases, τ_3/τ_{FP} is between 1.05 and 1.10. These six peaks are grouped into two groups, corresponding to two unstable period-3 orbits, which are labeled by an additional index 1 or 2 (Fig. 2).

We see that if the hole is placed at a position visited by an unstable periodic orbit of low period, in the case of the lo-

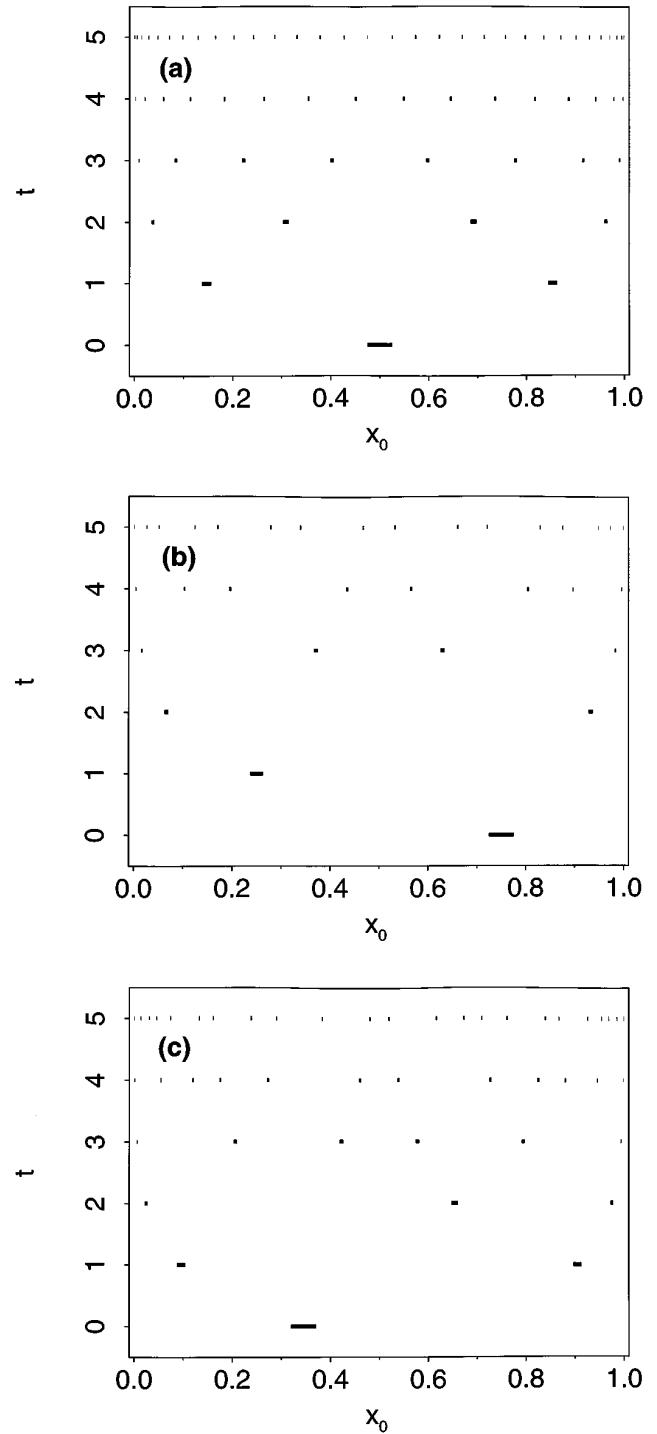


FIG. 3. Time maps for chaotic transients corresponding to map (1) with the hole position ξ equal to (a) 0.5, (b) 0.75, and (c) 0.345. The width of the hole is $d=0.1$. (In order to get clear visual presentation, this value is ten times larger than that used in other calculations in this paper.) (b) and (c) correspond to the two most pronounced peaks in Fig. 2.

gistic map at $r=4$, the average lifetime of the corresponding transient orbit for the map (1) is prolonged. This means that the hole at the position of an unstable periodic orbit acts in such a way as to prolong the wandering of transiently chaotic orbit on the unit interval; thus, inserting a narrow hole into the logistic map at $r=4$ may serve as a probe to test the

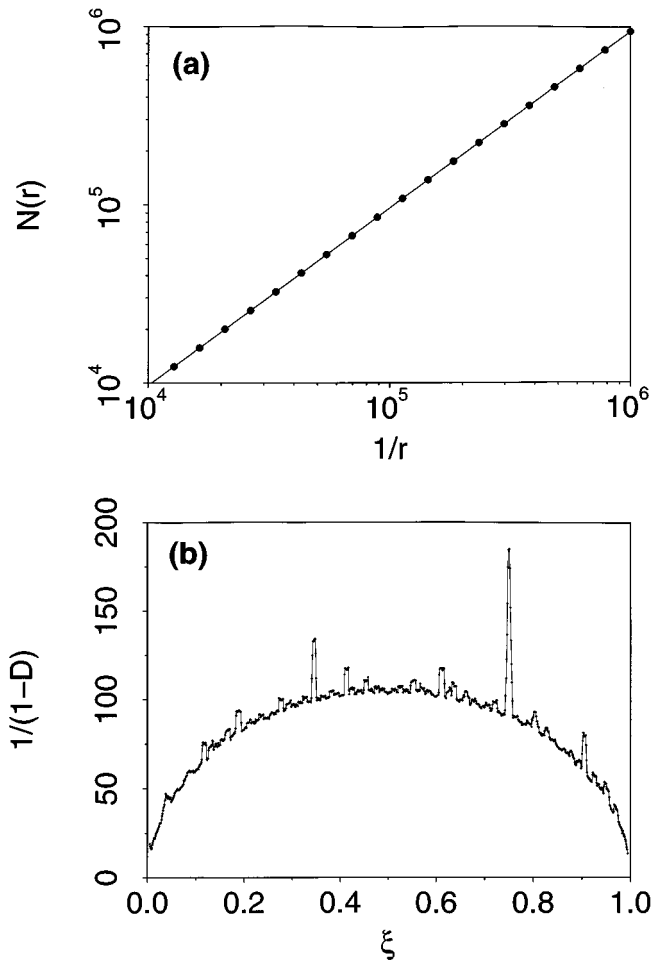


FIG. 4. Fractal dimension of the chaotic repeller associated with map (1). (a) Determination of the fractal dimension as the slope of the log-log plot of $N(r)$ vs $1/r$ for $\xi=0.75$, $d=0.01$. The slope is $D=0.99452 \pm 0.00005$. (b) Fractal dimension D of the repeller in dependence on the hole position ξ . The vertical axis displays $1/(1-D)$. It is seen that the graph $1/(1-D)$ vs ξ is practically identical to the graph τ vs ξ in Fig. 2.

positions of low-period, unstable periodic orbits.

Let us now explain this pattern. If the hole is placed at the position of the logistic map at $r=4$, the number of preimages and, consequently, the total width of all preimages are reduced, and fractal dimension of the repeller becomes larger, i.e., closer to unity. Then, according to the Kantz-Grassberger relation, the orbit will spend more time in the vicinity of the repeller, i.e., the average lifetime of the transient will be longer.

In order to elaborate this explanation, let us first investigate the structure of transient time maps (Fig. 3), which present lifetimes of individual trajectories, expressed in the number of iteration steps, for 10^6 initial points uniformly distributed along the unit interval.

Let us now consider the time map corresponding to $\xi=0.5$; in this case, the average lifetime is close to τ_{FP} . Trajectories starting in $I^{(0)}$ escape the unit interval in the first step, corresponding to lifetime $t=0$. The two first-order preimages of $I^{(0)}$, denoted by $I_1^{(1)}$ and $I_2^{(1)}$ in Fig. 1(a), correspond to the lifetime $t=1$. In general, the maximum number of preimages of n th order in Fig. 3(a) is $N_n=2^n$, each having

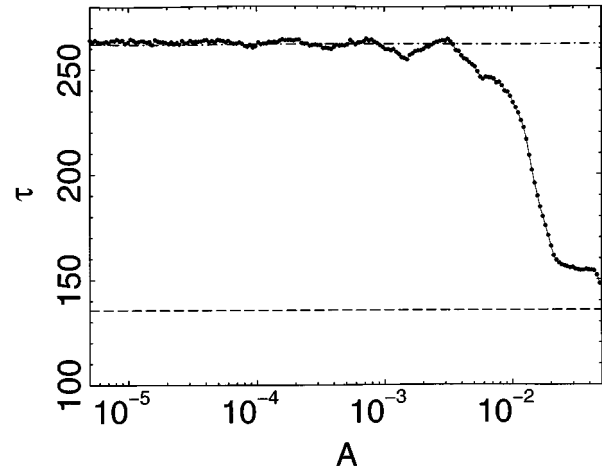


FIG. 5. Dependence of average lifetime τ of the largest peak in Fig. 2 (corresponding to the hole position $\xi=0.75$) on the amplitude of noise added on the r.h.s. of the logistic equation in map (1). For comparison, the predictions of the Frobenius-Perron (dashed line) and Kantz-Grassberger equation (dot-dashed line) without external noise are presented.

lifetime $t=n$ in analogy to previously studied single-humped maps [1,8].

For higher values of n some of the expected 2^n preimages are missing, as are those which accidentally fall in the interval $I^{(0)}$. For example, the number of $n=5$ preimages is not $2^n=32$, but it is equal to 30. Obviously, the number of the n th-order preimages approaches 2^n as the width of the hole diminishes.

In the limit of small hole width $d \ll 1$ the average lifetime can be approximately related to N_n by

$$\tau^{-1} \approx \sum_{n=1}^{\infty} \alpha_n N_n, \quad (3)$$

where N_n is the number of preimages of the n th order and α_n is a coefficient. In cases where $N_n=2^n$ (such as, for example, $\xi=0.5$ [Fig. 3(a)]), the average lifetime (3) approximately corresponds to the Frobenius-Perron prediction and is labeled by τ_{FP} ,

$$\tau_{FP}^{-1} \approx \sum_{n=1}^{\infty} \alpha_n 2^n. \quad (4)$$

On the other hand, for a peak at $\xi=0.75$, at the position of unstable periodic orbit of period $k=1$ [Fig. 3(b)], we have approximately $N_n=2^{n-1}$, which, after insertion into (3) and using (4), leads to an approximate expression

$$\tau_1 \approx 2 \tau_{FP}. \quad (5)$$

In general, for the peaks at positions corresponding to the unstable periodic orbits of period k , we get approximately

$$N_n = \begin{cases} 2^n, & n < k \\ 2^{n-k}(2^k - 1), & n \geq k \end{cases} \quad (6)$$

which leads to

$$\tau_2 \approx \frac{4}{3} \tau_{FP}, \quad \tau_3 \approx \frac{8}{7} \tau_{FP}, \quad \dots, \quad \tau_k \approx \frac{2^k}{2^k - 1} \tau_{FP}. \quad (7)$$

The true value of the number of preimages is slightly smaller than the estimate (6) because one should deduce those preimages which fall on $I^{(0)}$.

The average lifetimes τ_1 , τ_2 , and τ_3 obtained by direct calculation from exponential decay of trajectories are rather close to these values. The smaller the hole width d , the closer directly calculated average lifetimes are to the above estimates. For example, for $d=0.0001$, we get by direct calculation $\tau_1=2.000\tau_{FP}$ for the peak classified as $k=1$, and $\tau_2=1.331\tau_{FP}$ for two peaks classified as $k=2$. These values are very close to $\tau_1=2.000\tau_{FP}$ and $\tau_2=\frac{4}{3}\tau_{FP}=1.333\tau_{FP}$, given by Eqs. (5) and (7), respectively.

From each transient time map we can determine the corresponding fractal dimension D of the chaotic repeller by using a method similar to the one that was used in analyzing the winding number for the circle map in mode-locked intervals [24]. Accordingly, we present the log-log plot of $N(r)=[1-S(r)]/r$ vs $1/r$, where $S(r)$ is the total width of all preimages that are larger than a given scale r . Therefrom we get, for example, $D=0.9945$ for $\xi=0.75$, $d=0.01$ [Fig. 4(a)]. In Fig. 4(b), the dependence of the calculated values of $1/(1-D)$ (where D is the fractal dimension) on the hole position ξ is presented, keeping the width $d=0.01$.

On the other hand, the Lyapunov exponent is almost independent of the position of the hole, ξ being equal to the value $\lambda=\ln 2$, which corresponds to the $r=4$ logistic equation.

Inserting these calculated fractal dimensions and Lyapunov exponent into the Kantz-Grassberger equation [15]

$$\tau = \frac{1}{\lambda(1-D)}, \quad (8)$$

we obtain the average lifetime τ dependencing on the hole position ξ . This result coincides with Fig. 2, which was obtained by direct calculation of τ from the exponential decay of trajectories. Thus, the solid line in Fig. 2, in fact, corresponds to the Kantz-Grassberger equation.

The average lifetimes $\tau_1, \tau_2, \tau_3, \dots$ correspond to the Kantz-Grassberger lifetimes [Eq. (8)]. Equations (5) and (7), therefore, represent the relations between the Kantz-Grassberger and Frobenius-Perron average lifetimes.

We have further investigated the relation between Kantz-Grassberger and Frobenius-Perron predictions by adding noise to the r.h.s. of the map (1). In Fig. 5, the average lifetime τ , expressed in the number of iteration steps for $\xi=0.75$ dependent on the noise amplitude is presented. For comparison, the values of τ corresponding to Kantz-Grassberger and Frobenius-Perron predictions in the absence of noise are displayed. Calculation shows that the $\xi=0.75$ peak of τ is rather stable against noise up to the noise amplitude $\approx 10^{-2}$. However, with further increase of the noise amplitude there is a rapid reduction of τ from the value corresponding to the Kantz-Grassberger value τ_1 towards the lower value, corresponding to the Frobenius-Perron equation $\tau_{FP} \approx \frac{1}{2}\tau_1$, i.e., the peak is gradually washed out. Stability of the average lifetime below the threshold of noise is in accordance with previous indications that transients seem to be stable against noise [1,15], while the noise-induced destruction of peaks above the threshold of noise may be associated with the noise-induced chaos [25].

-
- [1] See, e.g., T. Tel, in *Directions in Chaos*, edited by Hao Bai-lin (World Scientific, Singapore, 1990), Vol. 3, p. 149, and references therein.
 - [2] J. L. Kaplan and J. A. Yorke, *Commun. Math. Phys.* **67**, 93 (1979); J. A. Yorke and E. D. Yorke, *J. Stat. Phys.* **21**, 263 (1979).
 - [3] T. Shimizu and N. Morioka, *Phys. Lett. A* **69**, 148 (1978).
 - [4] E. N. Lorenz, *Physica D (Amsterdam)* **13**, 90 (1984).
 - [5] J. Coste, *J. Stat. Phys.* **23**, 512 (1980).
 - [6] P. Manneville, *Phys. Lett. A* **90**, 327 (1982).
 - [7] F. M. Izrailev, B. Timmermann, and W. Timmermann, *Phys. Lett. A* **126**, 405 (1989).
 - [8] R. Artuso, E. Aurell, and P. Cvitanović, *Nonlinearity* **3**, 325, 361 (1990); **3**, 361 (1990).
 - [9] M. Franaszek, *Phys. Rev.* **46**, 6340 (1992).
 - [10] A. Csordas, G. Györgyi, P. Szeplafusy, and T. Tel, *Chaos* **3**, 31 (1993).
 - [11] P. Holmes, *Philos. Trans. R. Soc. London Ser. A* **292**, 419 (1979).
 - [12] J. P. Crutchfield and K. Kaneko, in *Directions in Chaos* (Ref. [1]), Vol. 1, p. 272.
 - [13] D. K. Umberger, C. Grebogi, E. Ott, and B. Afeyan, *Phys. Rev. A* **39**, 4212 (1989).
 - [14] C. Grebogi, E. Ott, and J. A. Yorke, *Phys. Rev. Lett.* **50**, 935 (1983).
 - [15] H. Kantz and P. Grassberger, *Physica D (Amsterdam)* **17**, 75 (1985).
 - [16] T. Bohr and D. Rand, *Physica D (Amsterdam)* **25**, 387 (1987).
 - [17] T. Bohr and T. Tel, in *Directions in Chaos* (Ref. [1]), Vol. 2, p. 194.
 - [18] P. Cvitanović, *Phys. Rev. Lett.* **61**, 2729 (1988).
 - [19] H.-O. Peitgen, H. Jürgens, and D. Saupe, *Chaos and Fractals* (Springer, New York, 1993).
 - [20] E. Ott, *Chaos in Dynamical Systems* (Cambridge University Press, Cambridge, 1993).
 - [21] R. M. May, *Nature* **261**, 459 (1976).
 - [22] M. J. Feigenbaum, *J. Stat. Phys.* **19**, 25 (1978).
 - [23] *Universality in Chaos*, edited by P. Cvitanović (Hilger, Bristol, 1984).
 - [24] M. H. Jensen, P. Bak, and T. Bohr, *Phys. Rev. A* **30**, 1960 (1984).
 - [25] R. L. Kantz, *J. Appl. Phys.* **58**, 424 (1985).